Acoustic admittance of organ pipe jets

S. Thwaites and N. H. Fletcher
Department of Physics, University of New England, Armidale, New South Wales 2351, Australia

(Received 25 November 1982; accepted 28 March 1983)

The admittance of a turbulent jet as the generator in organ flue pipes was investigated experimentally with respect to the relevant parameters, that is, the frequency, the jet efflux velocity, the mouth end-correction, and the jet tip deflection at the edge. First, an experiment was performed using a jet with a pulsating velocity to drive a pipe to isolate and identify the various drive mechanisms occurring in the jet-pipe interaction. The two established drive mechanisms, momentum drive and volume drive, were found to be operating, but the relative proportion of momentum drive was greater than expected. Turning then to a typical flue pipe arrangement, as a preliminary experiment, the jet admittance in the pipe was shown to be independent of the jet tip deflection so long as the deflection was less than about 0.7 jet widths. This constant admittance regime was then used to facilitate measurement of the pipe excitation as a function of the three remaining parameters. The admittance magnitude and phase were used, in conjunction with a knowledge of the jet behavior, to quantify the relative importance of the two drive mechanisms here, revealing once again a greater proportion of momentum drive than expected. To a good approximation, the admittance magnitude multiplied by the efflux velocity, and the admittance phase were each found to lie on a universal curve when plotted against a parameter consisting of the frequency divided by the efflux velocity, provided the cutup was constant. A deviation from expected behavior, as yet to be explained, was found in the jet admittance and phase for very low frequencies and high blowing pressures.

PACS numbers: 43.75.Np, 43.25.Sr, 43.28.Ra, 43.85.Bh

INTRODUCTION

The jet drive in organ flue pipes is a problem which has attracted considerable attention over the past decade and these efforts have lead to a great advance in understanding.[1–10] Nevertheless, a number of aspects of the interaction between the jet and the pipe are not well understood, and it is a series of experiments designed to investigate these which forms the subject of this paper. The problem, if treated from a fundamental starting point, has proven impossibly difficult, at least without further experimental evidence, since it involves the very complex fluid dynamical interaction between the jet and the standing wave at the edge. It is, however, still possible to progress from an empirical standpoint towards a better description.

The jet and the pipe are thought to interact according to two mechanisms. These were originally proposed, very qualitatively, by Helmholtz[11] and Rayleigh.[12] Experimental and theoretical attention to them since has confirmed their probable applicability and has gone some way to elucidating them in more detail. The two mechanisms are known as "volume drive" and "momentum drive." They are best described in terms of the analog electrical circuits proposed by Elder[3] for a pipe sounding normally, shown in Fig. 1.

Volume drive, depicted in Fig. 1(a), involves the injection of the jet fluid into the standing wave on or about times of maximum compression at the driving point. As such, the jet "sees" the parallel impedance of the pipe Z_p and of the mouth Z_m, and the flow in the pipe Q_p is simply the sum of the jet flow Q_j and the mouth flow Q_m.

For momentum drive, depicted in Fig. 1(b), the pipe is driven by the pressure Δp, generated by the jet as it slows and spreads in the pipe. The accepted general form of Δp is given in the figure where S_p is the cross-sectional area of the pipe, S_j is the jet area in the pipe, v_0 is the jet efflux velocity, and ρ is the density of air. This interaction occurs at times of maximum fluid velocity in the pipe and involves the transfer of the jet momentum, effecting an acceleration of the pipe fluid. The jet flow does not contribute to the pipe flow, resulting in a pipe flow which is equal to the mouth flow. The equations from these circuits giving the form of the pipe flow in terms of the jet flow are shown on the figure.

Now, it is evident that both these descriptions are sim-

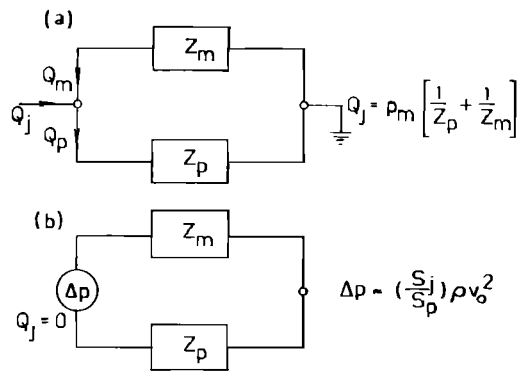

FIG. 1. The electrical analog circuits representing the two drive mechanisms, as portrayed by and with the sign conventions of Elder. (a) Volume drive. The jet sees the parallel combination of the jet and mouth impedances, and the jet and mouth flows add to produce the pipe flow. (b) Momentum drive. In slowing and spreading, the jet transfers its momentum to the pipe flow. The pressure created just inside the mouth by the jet is given by Δp and the pipe flow equals the mouth flow.

 0001-4966/83/080400-09$00.80 © 1983 Acoustical Society of America

plistic but that insofar as they exist, they probably both occur in the overall interaction. Theoretical studies on a hypothetical experiment where the pipe is driven by a stationary jet with pulsating velocity were performed by Elder[3] who found terms in his solution resembling both drives together with other nonlinear terms. Fletcher[7] postulated a jet of constant velocity and with a tophat profile, which was deflected in and out of the pipe giving a jet flow variation into the pipe dependent on the jet area intersected by the lip. For this arrangement he also found two terms like those already described plus small nonlinear ones. In a later paper Fletcher[8] showed that a convenient way to write these two terms is in the form of a drive equation giving the pipe flow Q_p, in terms of the jet flow Q_j. Remembering that the mouth impedance may be written $Z_m = j\rho\omega\Delta l/S_p$, where Δl is the end correction at the mouth and ω the angular frequency, this drive equation is

$$Q_p \simeq \{[\rho(v_0 + j\omega\Delta l)/S_p]/(Z_p + Z_m)\}Q_j, \quad (1)$$

where v_0 is the jet velocity at the flue. As was evident from their description, the two drives are $\pi/2$ apart in phase.

If the magnitudes of the two terms are calculated using typical pipe parameters and frequencies, then we find $\omega\Delta l \gg v_0$, suggesting that volume drive is the more important mechanism. For volume drive, considerations of the feedback involved to the jet suggest that the phase delay necessary on the jet to complete the loop is π, that is, one half-wavelength. Coltman[5] found one half-wavelength on the jet in his experiments involving a pipe sounding at resonance. The pipe configuration he used, and the frequency, were indeed such as to set Eq. (1) well over into the volume drive regime.

Coltman[13] has also performed an experiment explicitly designed to isolate and measure the two drives. It involves the use of a pulsating jet as envisaged by Elder[3] to drive a pipe, open at both ends, at its center. This arrangement was based on the rationale that volume drive in the pipe should not vary with the direction of the jet while momentum drive is essentially a vector interaction. Thus, for a pipe driven at its center at the frequency of the second pipe mode, a reversal of the jet direction in the pipe should produce no reversal of phase of the pipe excitation for volume drive and a reversal of π for momentum drive. In addition, volume drive at the center will produce only a weak excitation since the two pipe halves will vibrate π out of phase, with a pressure node at the drive point and thus a very small driving point impedance. For momentum drive the two halves must vibrate in phase, at the natural resonance of the pipe, so the excitation is strong.

Coltman found evidence of momentum transfer as well as volume drive with this arrangement, but its dependences, in both magnitude and phase, on the center line flow velocity were not as expected.

I. EXPERIMENT WITH A PULSATING JET

Although a jet with a pulsating velocity is not really at all like the oscillating jet in real organ pipes, the thought experiment devised by Elder is still of interest and of possible use. Therefore, an apparatus was constructed along very similar lines and some simple experiments done to try to isolate and quantify the two drives.

This apparatus, shown in Fig. 2, consists of a 2-m pipe of 10-cm diameter, open at both ends, which is driven at one end by a pulsating axisymmetric jet. The pulsations were produced using a 23-cm-diam loudspeaker which fed into a small cavity via a 2.0-m inverted exponential horn. The small cylindrical cavity, 2.5×15 cm, was fed at one end from the compressed air supply and the jet nozzle was connected to the other. The jet nozzle, an aluminum tube 3 mm in diameter and about 30 cm long, was bent into a right angle so that the cavity and other parts did not materially affect the end correction of the pipe. The efflux pressure was measured with a pitot tube connected to a pressure transducer and meter. The signal from the transducer, when displayed on an oscilloscope, showed both the steady pressure and the ripple. The pipe was always driven at resonance, 87 Hz, and was mounted on a traversing mechanism so that the jet blowing position could be varied. The acoustic pressure p_p, in the pipe and thus the drive, was monitored with a $\frac{1}{4}$-in. condenser microphone inserted into the pipe wall at the position of the pressure antinode, half way along.

The rationale for this arrangement is simple. We write the efflux pressure as $P + \tilde{p}$, where P is the steady pressure and $\tilde{p}$ is the fluctuating pressure. If $\tilde{p}$ is always small compared to P then we may write the efflux velocity v, as

$$v \simeq (2/\rho)^{1/2}(P^{1/2} + \tfrac{1}{2}\tilde{p}/P^{1/2}). \quad (2)$$

Now substitutions can be made into Eq. (1) for v_0 and Q_j where we write $v_0 \propto (2/\rho)^{1/2}P^{1/2}$ and $Q_j \propto (2/\rho)^{1/2}(\tilde{p}/P^{1/2})$.

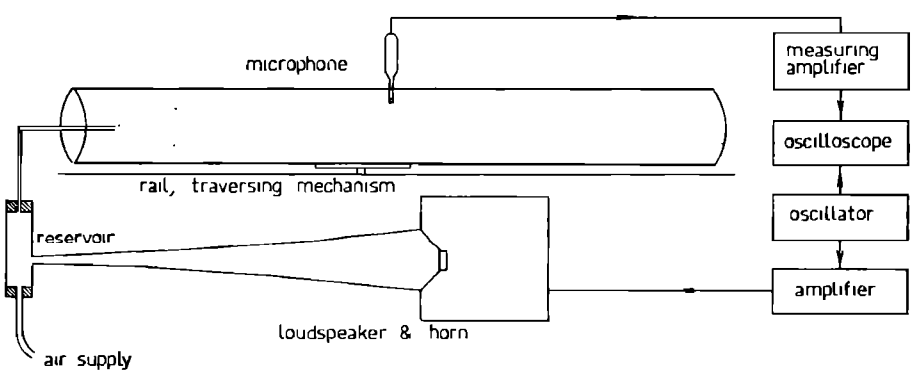

FIG. 2. Schematic diagram of the apparatus used to measure the excitation of a pipe driven by a pulsating jet.

With the added simplification of the use of two constants, C_1 and C_2, Eq. (1) becomes

$$Q_p \propto C_1(C_2 + j\omega\Delta l/P^{1/2})\tilde{p}. \quad (3)$$

Thus both drives are proportional to $\tilde{p}$ but their ratio varies as $P^{1/2}$. The experiment simply involves ascertaining the variation of the excitation in the pipe, p_p or Q_p, as a function of P for various values of Δl as controlled by the position of the jet nozzle.

Δl was measured from the virtual pressure node, measured to be 2 cm outside the pipe. The values of Δl used were $\Delta l = 1$, 8, and 13 cm. The results are plotted in Fig. 3(a). The data set for $\Delta l = 8$ cm was fitted with Eq. (2) yielding $C_1 = 4.5$ and $C_2 = 3.4$ in SI units. This same equation was then plotted for the other Δl values. All three curves are shown in the figure and the agreement is good. From the value of C_2 we find that a coefficient of 2.6 before the v_0 term in Eq. (1) correctly adjusts the relative magnitudes of the drives for this situation.

The phase shift in the pipe excitation as we move from one blowing position to another can also be predicted from Eq. (3). Unfortunately, at $\Delta l = 1$ cm the nozzle is outside the pipe and the spherical nature of the wave fronts here complicates the answers, but between $\Delta l = 8$ cm and $\Delta l = 13$ cm a complete set of phase shifts, as a function of P, can be obtained. These are shown in Fig. 3(b) and again agreement with Eq. (3) is reasonable. The theoretical predictions in Eq. (2) are contingent on $\tilde{p}$ being very small.

II. THE JET TIP DEFLECTION

We turn now to the real problem at hand, the jet drive in an organ pipe. In all the following the x coordinate measures distance along the jet and the y coordinate distance across the jet's short dimension. The origin is at the slit. The various characteristics of wave propagation on plane turbulent jets will be referred to constantly in the following so we summarize them here.[14–16]

The center line velocity $v(x,0)$, of a plane turbulent jet varies simply as

$$v(x,0) = C(x - 3h)^{-1/2}, \quad (4)$$

for $x > 3h$, where h is the slit width and C is a constant which depends on v_0. The jet profile can be well described by the relation

$$v(y) = v(0)\mathrm{sech}^2(y/b), \quad (5)$$

where b is the jet width which increases linearly with x. The phase velocity of disturbances on this jet $u(x)$, is given well enough by $v(x)/2$. The disturbances grow approximately as $\cosh G(x)$, where $G = \int_0^x \mu(x)dx$ and μ is the growth parameter. The theoretical form of μb for plane laminar jets has been calculated, as a function of kb, where $k = \omega/\mu$ is the wavenumber, by various numerical methods. Previous experiments[16] have shown that the disturbance growth on plane turbulent jets is well described by a similar result. For our purposes the form of $\mu b\,(kb)$ is adequately given by the equation

$$\mu b\,(kb) \simeq 0.9[1 - \exp(-3kb)] - 0.45kb. \quad (6)$$

The measurements in this section were done in terms of the jet admittance Y_j, defined as the ratio of the resultant flow generated in the pipe Q_p, to the particular applied pressure, p_p. An admittance representation was chosen on the basis of certain expectations about the answers. The pipe, represented by a transmission line, was seen to be terminated by a parallel combination of the jet admittance and the mouth admittance, as shown in the circuit in Fig. 4(a). Evidently this circuit is similar to the one in Fig. 1(a) showing volume drive. As we have already seen, this particular arrangement causes the pipe flow to be divided between the two admittances according to their relative magnitudes. Already this is patently simplistic, since the jet behavior is dependent on the mouth flow, after a fashion, and not strictly on the pipe pressure. Nevertheless, it is a circuit to go on with.

The jet admittance was obtained by subtracting from the total measured admittance the admittance with the jet turned off. A standing wave ratio technique was used. As shown in Fig. 4(b), the 2-m pipe of 10-cm diameter was equipped at one end with a perspex foot having a flue 4 cm long and 0.5 mm wide. The cutup d was 1 cm and the mouth width was 4 cm. The flue was positioned so that the jet blew in a plane 1 mm outside the mouth. Thus the jet was not symmetrically intercepted by the lip. This foot and flue, when connected to the appropriate resonator, functioned as a normal organ pipe. The jet efflux pressure was measured with a pitot tube connected to a pressure transducer. This was used to calibrate a pressure gauge connected to the foot.

The sound was injected about 30 cm from the open end through a 2.5-cm hole. The loudspeaker arrangement depended on the experiment. For large acoustic displacements

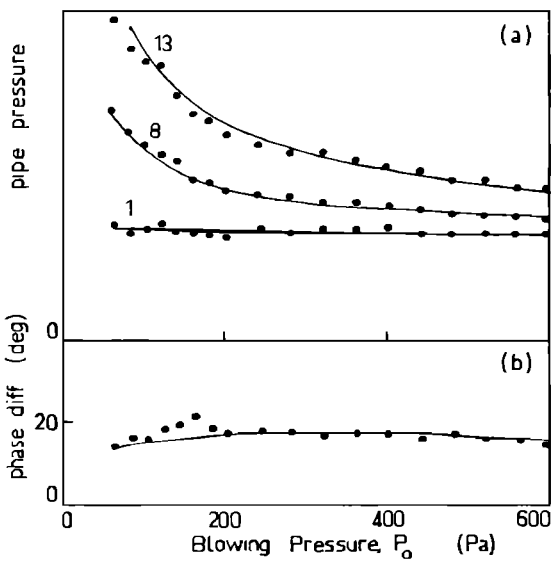

FIG. 3. (a) The form of the pressure generated in the pipe driven by a pulsating jet, measured as a function of the steady blowing pressure, P, for the three end corrections, Δl, shown in centimeters. The solid lines give the form of Eq. (3). The pressure is given in arbitrary units. (b) The phase difference, in degrees between the pipe excitation at $\Delta l = 8$ cm and $\Delta l = 13$ cm, measured as a function of P. The solid line shows the theoretical form of this, calculated from Eq. (3).

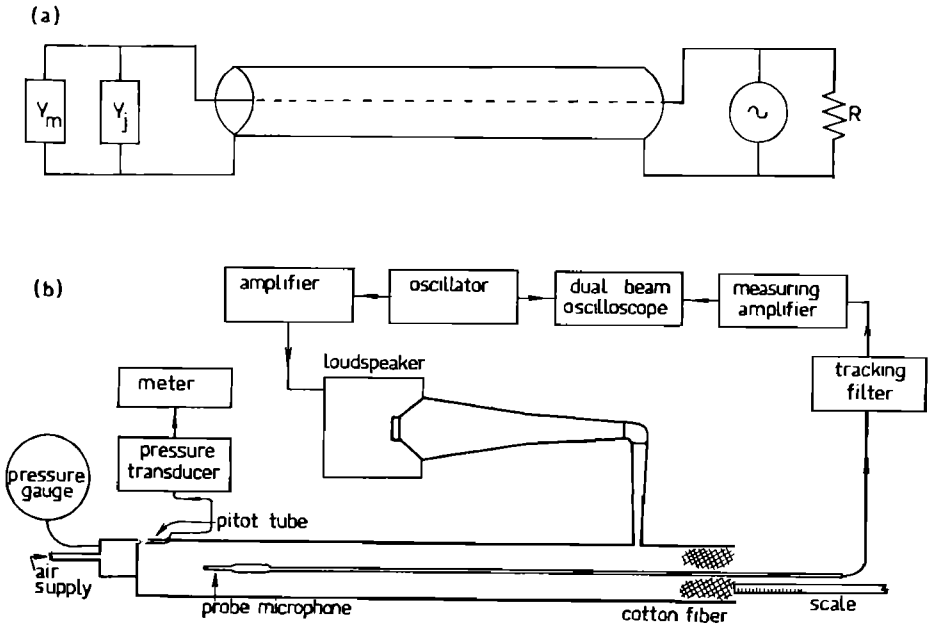

FIG. 4. (a) The equivalent circuit representing the organ pipe in the standing wave experiment. The transmission line representing the pipe is terminated by the parallel combination of the jet and mouth admittances, Y_j and Y_m. The loudspeaker generator and the acoustic resistance R, representing the sound absorbent cotton are shown at the other end. (b) Schematic diagram of the apparatus used to measure the jet admittance.

the inverted exponential horn arrangement from Sec. I was used, as shown in the figure. For small displacements, where a good frequency response was generally required, a good quality 10-cm speaker in a simple, cotton-packed wooden box was used.

The wave thus generated travels to the mouth end and is reflected, undergoing changes in both magnitude and phase as a result of the admittance of the reflector, in the process. The reflected wave travels back to the open end and is largely absorbed by a wedge of cotton placed there for that purpose. In this way the feedback loop between the jet and the standing wave in the pipe, necessary for self-sustained oscillations, is incomplete and the jet excitation is under the control of the experimenter. The incident and reflected waves combine to form a standing wave whose ratio of maximum to minimum pressures, the standing wave ratio, and distance to the first minimum, allow the terminating admittance of the pipe to be calculated. The distance to the first minimum was measured from the surface of the languid so that the calculated admittances are for an assumed interaction on this plane. The requisite equations are well known,[17] the one modification being that if the jet is driving the pipe the admittance is generating rather than dissipative and the real part of Y, Y_R, is negative. The equations are ambiguous with respect to the sign of Y_R.

The standing wave was probed with a $\frac{1}{4}$-in. B and K condenser microphone mounted at the end of a 2-m probe. Its associated electronics are shown in Fig. 4. The sign of Y_R was determined from the direction of the phase shift in the standing wave as the microphone was traversed through a minimum.

Now from Eq. (1) we can see that the important variables in determining the relative drive magnitudes are ω,v_0, and Δl. There are, however, other variables which must be controlled and the most vital of these is the jet deflection at the edge, D.

The magnitude of the drive is a nonlinear function of the jet tip deflection. When the jet tip deflection is small the resultant jet flow into the pipe increases almost proportionally with D but, when D is large, further increases cause no increase in Q_j since the jet is already swinging fully into and out of the pipe. This saturation condition is known as complete switching of the jet. Although the phase velocity and growth of waves is quite well understood from previous experiments,[15,16] the accuracy of predicted tip deflections from these data is not adequate to eliminate these effects from the problem. This difficulty can be quite easily avoided by the use of very small deflections where Q_j is roughly proportional to D, since this is the same as saying that at small deflections the jet admittance is constant, independent of the deflection.

This result was established experimentally, giving in the process an indication of the typical deflections produced in our pipe and the limiting deflection for a roughly constant admittance. The jet admittance was measured as a function of the jet tip deflection, D, with ω, v_0, and Δl all constant. The jet deflection at the edge was measured using an identical technique to the one used to investigate disturbance growth in a previous paper.[16] The frequency chosen was as low as practicable because large deflections, up to twice the jet width at the edge, were required. Since the mouth admittance varies as $1/\omega$, the mouth flow varies as $1/\omega$ if the pipe pressure is held constant. The acoustic displacement in the mouth ξ_m, varies as Q_m/ω, so that $\xi_m \propto 1/\omega^2$. Thus for large ξ_m we want small ω. The inverted acoustic horn also aided in the production of large displacements. The chosen frequency was 125 Hz.

The measured jet admittance Y_{j_1}, at the fundamental is shown plotted in Fig. 5(a). It may be argued on the basis of jet measurements reported earlier,[16] that the jet deflection D, is proportional to ξ_m and in turn to p_p, the pipe pressure. Thus the form of the flow Q_p, is simply given by $Y_{j_1} D$. We may

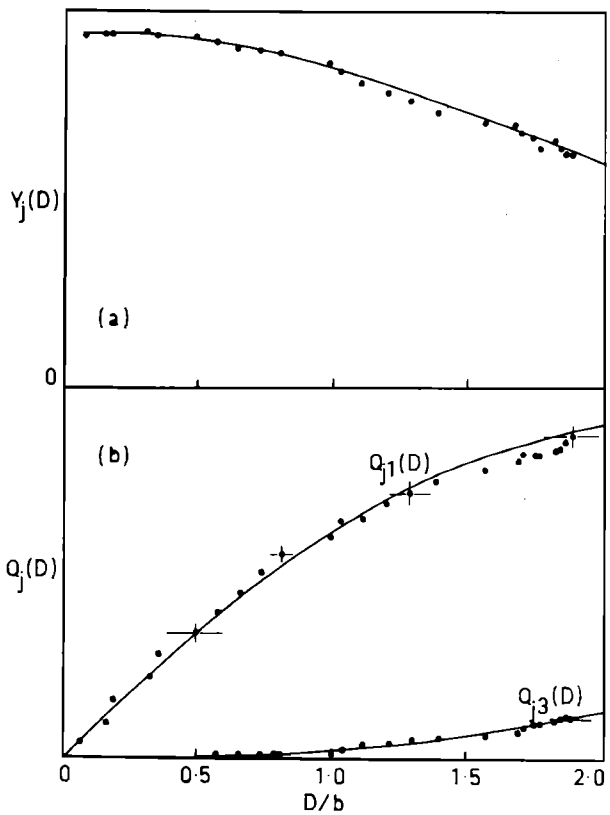

FIG. 5. (a) The measured form of the jet admittance Y_j as a function of the jet deflection D. The solid line is the theoretical result from Eq. (7). (b) The form of the measured flow into the pipe for the fundamental Q_{j_1} and the third harmonic Q_{j_3} as a function of the deflection D. The solid lines are the theoretical result calculated using Eq. (7). In these graphs the vertical scales are arbitrary.

further infer that this is also the form of Q_{j_1} since Eq. (1) shows that $Q_p \propto Q_j$ provided ω, v_0, and Δl are constant, which they are for this experiment. The form of Q_{j_1} obtained in this way is shown in Fig. 5(b).

When the deflection is small, the flow Q_{j_1} increases roughly proportionally with D which means that the ratio Q_p/p_p (which is proportional to Q_j/D) is nearly constant, that is Y_{j_1} is nearly constant. For larger deflections, Q_{j_1} does not increase so rapidly and for very large D, that is complete switching of the jet, $Y_{j_1} \propto 1/D$.

The theoretical forms of these curves can be calculated quite easily.[10] If the jet tip is oscillating sinusoidally and has an offset, or asymmetry with respect to the edge of y_0, then its displacement is simply $y(t) = -(y_0 + D \sin \omega t)$. Using Eq. (5) for the jet profile, the form of the jet flow into the pipe is given by

$$Q_j = \int_{-\infty}^{-y_0 - D\sin\omega t} y(t)\,dy$$

$$= v_0\{1 - \tanh[(y_0 + D\sin\omega t)/b]\}. \quad (7)$$

The forms of Q_j at the fundamental and at the various harmonics can be obtained from this by Fourier analysis.

The theoretical forms of Y_{j_1} (proportional to Q_{j_1}/D) and Q_{j_1} are plotted in Fig. 5(a), (b) for comparison with the experimental results. The agreement is good. Of course the ordinates have been adjusted with an appropriate multiplicative constant. Also plotted in Fig. 5(b) is Q_{j_3}, the third harmonic generated in the pipe by the fundamental on the jet as calculated from Eq. (7). The experimental results for this were simply obtained by measuring the pressure amplitude in the pipe generated at three times the driving frequency. Note that this wave is not a standing wave but a traveling wave generated at the mouth and absorbed at the open end in the cotton.

These results show that there is a reasonably wide low-deflection regime, $D \lesssim 0.7b$, where we need not be troubled by nonlinear effects, and where the jet admittance is not dependent on the deflection.

III. THE JET ADMITTANCE EXPERIMENTS

We now proceed to describe a set of measurements of Y_j involving ω, P_0 the efflux pressure, and Δl. The same apparatus was used as in the last section with the exception that the small loudspeaker, having a better frequency response but smaller displacement, replaced the larger one. It was connected to the hole in the pipe by a 20-cm length of 25-mm-diam plastic hose inserted into a face plate over the loudspeaker cone. In addition, the slit length was increased to 6 cm as this allowed smaller end corrections to be used, favoring the momentum drive term in Eq. (1). The slit width remained at $h = 0.5$ mm. As in Sec. II, the distances to the standing wave minima were measured from the plane of the languid.

Each experiment involved setting the values of P_0 and Δl and obtaining Y_j as a function of the frequency f, from $f = 100$ to 500 Hz at 50-Hz intervals. Δl was varied by either adding "ears" which increased it or by doubling the cutup, d, which decreased it. As an initial experiment, the mouth admittance Y_m, had to be measured since it was to be subtracted from the total admittance to give the jet admittance. The mouth admittance, as a function of f for each end-correction, proved to be very well behaved and predictable. The real part was small and the imaginary part varied almost exactly as $1/f$. The imaginary part was used to calculate the values of the end corrections for the three different mouth geometries. These were $\Delta l = 19$, 24, and 30 cm. The blowing pressures for the experiments were, for $\Delta l = 19$ cm, $P_0 = 200$, 400, 800, and 1500 Pa, for $\Delta l = 24$ cm, $P_0 = 100$, 200, 400, 800, and 1500 Pa, and for $\Delta l = 30$ cm, $P_0 = 400$, 800, and 1500 Pa.

When plotted as graphs of the real part of Y_j versus the imaginary part, the jet admittances produced spirals, much as expected. The results for $\Delta l = 24$ cm, $d = 1$ cm, and for $\Delta l = 19$ cm, $d = 2$ cm, are shown in Fig. 6(a),(b). The results for $\Delta l = 30$ cm, $d = 1$ cm, the pipe with ears, were very similar to those for $d = 1$ cm and no ears. The $d = 1$ cm and $d = 2$ cm results are startlingly different and we obviously have several interesting effects.

IV. THE JET-PIPE INTERACTION: PHASE

The phase of the jet admittance is the sum of the phase shift involved in the disturbance travel time on the jet δ_j, and the phase shift δ_p, between Q_p and Q_j, if any, introduced by

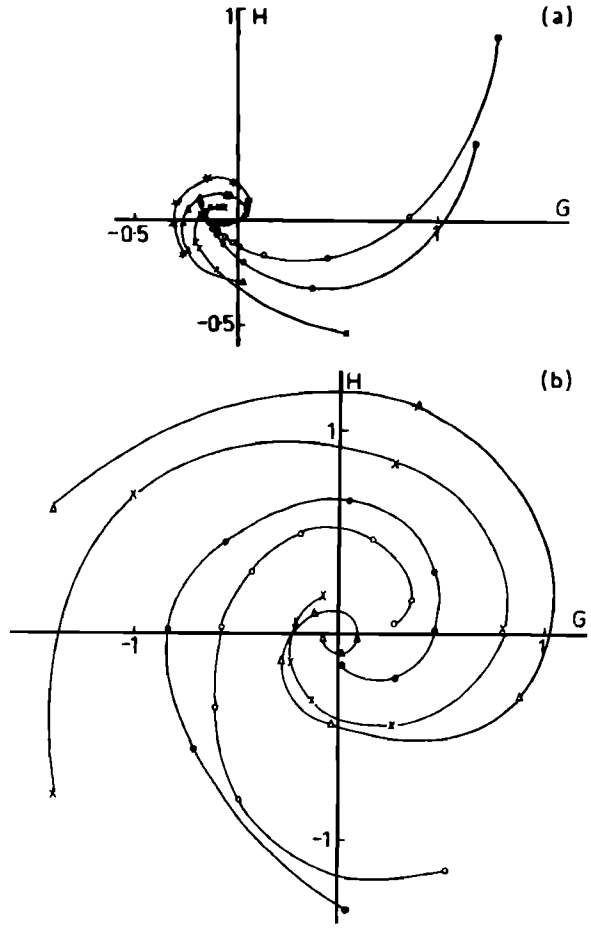

FIG. 6. (a) The measured jet admittance plotted as the real part versus the imaginary part for five different blowing pressures P_0. The cutup, $d = 1$ cm and the frequency increases in a clockwise direction around the curves, where the symbols show the measurement intervals 50 Hz apart over the range 100–500 Hz. (b) A similar set of jet admittance measurements where the cutup is now $d = 2$ cm and four different blowing pressures have been used. O-O-, $P_0 = 1500$ Pa; ●-●-, $P_0 = 800$ Pa; ×-×-, $P_0 = 400$ Pa; Δ-Δ-, $P_0 = 200$ Pa, and ∗-∗-, $P_0 = 100$ Pa.

the actual interaction. The frequency influences δ_j; δ_j is proportional to ω, and it also influences the relative sizes of the two terms, and thus δ_p, in Eq. (1). For blowing pressure P_0, $\delta_j \propto 1/P_0^{1/2}$, and again the relative magnitudes of the two terms in Eq. (1) are dependent on P_0. The effect of the cutup, d, seems a little more complex at first. The transit phase delay δ_j, varies as $d^{3/2}$. This comes from the appropriate integration of the disturbance phase velocity given in Eq. (4). d also influences Δl but not simply.

Clearly δ_j must be separated from δ_p if we are to learn anything of the jet-pipe interaction from the jet admittance. The jet displacement $y(t)$, at position x along its length, is given by

$$y(t) = (U_m/\omega)[\sin \omega t - \cosh G(x) \sin(\omega t - \delta_j')], \quad (8)$$

where $U_m \cos \omega t$ is the assumed acoustic particle velocity in the mouth.[8] The first term represents the bodily displacement of the jet in the acoustic field in the mouth and the second the displacement due to the wave growing on the jet. For large f and small P_0 the second term dominates in this equation, giving

$$y(t) \simeq -(U_m/\omega) \cosh G(x) \sin(\omega t - \delta_j'), \quad (9)$$

where

$$\delta_j' = (4/3C) d^{3/2} \omega.$$

In general, however, Eq. (8) may be rearranged into the form showing the transit phase more directly

$$y(t) = -(U_m/\omega)[1 + \cosh^2 G(x) - 2 \cosh G(x) \cos \delta_j']^{1/2} \times \sin(\omega t - \delta_j' - \pi/2) \quad (10)$$

where

$$\delta_j = \tan^{-1}[1 - \cosh G(d) \cos \delta_j'] / [\cosh G(d) \sin \delta_j']^{-1}.$$

In the light of the result in Eq. (9), the data in Fig. 6(a), (b) were replotted as admittance phase δ versus the parameter ω/v_0, shown in Fig. 7. Clearly all the points condense onto a single curve provided d is constant, as we might have hoped from the preceding remarks. We retain ω/v_0 as our parameter, rather than $\omega d^{3/2}/v_0$, because it will prove to have the greater usefulness. The $d = 2$-cm data would fall on the $d = 1$-cm curve were it scaled in the abscissa by the factor $2^{3/2}$. It was plotted separately, as shown, to avoid having to condense the points for $\omega/v_0 \lesssim 100$ towards the phase axis to such an extent that their behavior is not clear. The curves relating to the $d = 1$-cm data are the ones relevant to the ensuing discussion.

On the same graph is plotted, as the dark line, δ_j as

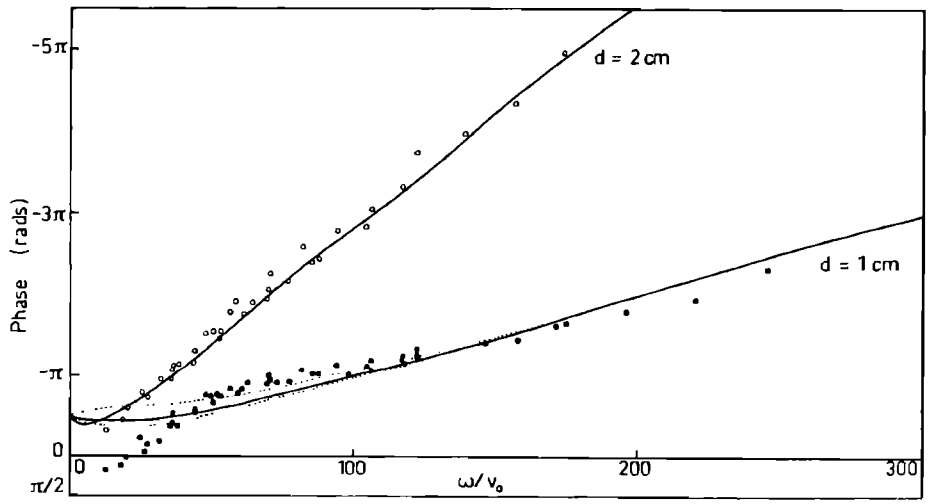

FIG. 7. The phase of the data from Fig. 6(a),(b) replotted as a function of ω/v_0. O-O-, $d = 2$ cm; ●-●-, $d = 1$ cm. The solid lines show the phase delay due to the jet motion δ_j, as given by Eq. (10). The dotted lines show the envelope of phases for the jet admittance calculated with Eq. (11).

given by Eq. (10). Over nearly all the range in the abscissa the data fall on or near this curve, suggesting that the admittance phase is hardly ever very different from the transit phase alone. However, for $\omega/v_0 \lesssim 100$, the data have progressively slightly larger delays and for $\omega/v_0 \lesssim 40$ the phase delay suddenly starts to decrease rapidly.

To examine these trends in the light of the drive equation, certain modifications need to be made to allow for the conditions peculiar to our experiment. Equation (1) was formulated for an organ pipe sounding at resonance and so the jet as a generator sees an impedance minimum. For this to be so the pipe impedance Z_p, in the denominator of Eq. (1) must have an imaginary part of equal size but opposite sign to Z_m. This gives a small and mostly real denominator.

In our case the pipe is not at resonance. It may be argued that the required form of Z_p is the characteristic impedance of the tube, $Z_0 = \rho c/S_p$. This can be seen by considering the standing wave in the pipe to be the sum of two waves, one generated by the speaker which travels to the mouth and, on reflection, travels back to be absorbed in the cotton, and the other a traveling wave generated by the jet which is also absorbed by the cotton. With this modification Eq. (1) becomes plausibly

$$Q_p \simeq \frac{[\rho(2.6v_0 + j\omega\Delta l)/S_p]}{[\rho c/S_p + j\rho\omega\Delta l/S_p]} Q_j, \tag{11}$$

where the factor 2.6 has been included from Sec. II. This equation is not strictly a function of ω/v_0, although as we shall see, this parameter retains its usefulness. The numerator has the added dependence on Δl and the denominator has no term containing v_0. Evidently the equation possesses a phase shift of $\pi/2$ in both the numerator and the denominator, from being largely real to largely imaginary, as ω increases.

Viewed in terms of our data this has many encouraging aspects. When ω is sufficiently large that both the numerator and the denominator are imaginary, the resultant pipe flow Q_p, is in phase with the jet flow Q_j. The drive is of the volume type and the admittance phase is given simply by Eq. (9) with an intercept at $\delta = 0$. It is thus quite apparent that we have volume drive in Fig. 7 whenever $\omega/v_0 \gtrsim 100$. Nearly all the data for $d = 2$ cm is in this regime, as would be more obvious had we included the factor $d^{3/2}$ in the abscissa.

The transitions in Eq. (11) to a situation in which both the numerator and the denominator have substantial real parts instead of being purely imaginary occur over similar ranges in ω/v_0 for the particular configuration of the experiment, and thus for typical organ pipes. In the numerator this transition represents a change to momentum drive. Should this take place without the corresponding shift in the phase of the denominator, a curve on Fig. 7 predicting the phase of the admittance would bend away from the solid line towards larger negative δ values, finally intersecting the axis at $\delta = -\pi$. Of course the phase shift in $Z_p + Z_m$ counteracts this, in some cases almost exactly so, leaving the solid line in the figure as the overall admittance phase.

For each combination of the values of ω, v_0, and Δl there is an admittance phase curve. When these are plotted in a diagram like Fig. 7 they form a set of curves, all of which conform to Eq. (10) for large frequencies and small blowing pressures. For $40 < \omega/v_0 < 100$ they deviate from this prediction, mostly towards more negative phases and, as ω/v_0 goes to zero, δ tends to a value of $-\pi/2$. The envelope of these curves, the phase of Q_p/Q_j in Eq. (11), is also plotted, as the dotted lines, along with Eq. (10) in Fig. 7.

For the middle section of the results, the curves in Fig. 7 suggest that momentum drive is occurring very much as described by Eq. (11). The phase shifts are of the right order, they are in the right direction and they occur over the right ranges in ω, v_0, and Δl. The factor of 2.6 in the momentum drive term is clearly necessary for this agreement. Whether this factor is a real reinterpretation of the momentum drive term or whether it really represents a reweighing of the two terms because of an erroneous interpretation of Δl, for instance, is not clear from our results. It is, perhaps, remarkable that this number, obtained from such a physically dissimilar arrangement as the pulsed jet, should be so reasonable in the current context. From the results in Fig. 7, it may be argued that the coefficient, 2.6, might be increased, by perhaps 50%, in the case of ordinary jet drive but it is not possible here to make a significantly better estimate of its exact size than this.

The remaining section of the data has $\omega/v_0 \lesssim 40$. Here the phase of the admittance suddenly becomes far less negative and even crosses the axis into positive values. It may be argued that this shift to positive phase is spurious and that the curve should intersect at $\delta = 0$. Although no reason is known which explains this low ω/v_0 behavior, a positive phase for the admittance would be even more difficult to account for than the one we already have. From the experimental scatter in the rest of Fig. 7 this phenomenon could be attributed to measurement uncertainty but, in performing the experiments, there is no doubt that the sign of these phases is as reported even if the magnitudes are uncertain.

When the admittance spirals were plotted, spirals for the series impedance circuit were also tried for some data sets. The spirals formed in this way were not nearly so well behaved, or illuminating, as in the admittance case and so the method was discarded. However, one general feature which emerged from the exercise was that the calculated jet impedances at low ω/v_0 where shifted by about 20° in the direction of larger negative phases. This is not a great amount but it is enough, in terms of the diagrams like Fig. 7, to cause the curve of data points to intersect the phase axis at $\delta = 0$. This does not mean that the impedance representation is the right one. Rather, it implies that the division of the currents between the two branches in Fig. 4(a) is not correctly determined by the admittances as defined there. One clearly possible mechanism which has not been included, explicit in Coltman's discussion of edgetones,[5] is that part of the jet flow into the pipe returns as backflow through the mouth. It is the opinion of M. E. McIntyre (personal communication) that the inclusion of this process is necessary to a full description of the fluid dynamics of the jet–edge interaction.

V. ADMITTANCE MAGNITUDE

Plainly, from the results plotted in Fig. 6(a),(b), the magnitude of the admittance generally decreases with increasing frequency and increases with increasing blowing pressure. It also appears that it increases as the cutup increases. As in the last section it is possible to replot the points from Fig. 6(a),(b) against the parameter ω/v_0 so that all the data condenses onto a single curve. The form of this curve will then show the sort of changes from one range to another in ω/v_0 consistent with the regimes of separate behavior found for the phase.

In order that the magnitudes all fall on the same curve, the data needs to be adjusted with respect to the ordinate to allow for the effects of both the cutup and the efflux pressure. The effect of the cutup may be eliminated by the following simple argument. Consider the case of two data sets having v_0 constant, ω increasing around the spirals, and different values of d. Along any radial line of constant phase intersecting the spirals, kb is the same function of x/d, the fractional distance along the jet, independent of d. As we saw in the discussion of the phase, in spite of all the various phase changes which might occur in the drive equation, for $\omega/v_0 > 40$ the phase of the admittance is never very different from the phase delay due to the travel time on the jet. If the radial sample is taken for data in the volume drive regime, this is a very good approximation.

As Eq. (6) shows, μb depends only on kb and is also a fixed function of x/d, which yields constant growth ($\mu x = \mu b \cdot x/b$) since x/b is constant. Thus the jet tip deflection D is in a constant ratio to the acoustic mouth displacement ξ_m, $D \propto -\xi_m$. Now for a constant pipe pressure p_p, as we have always maintained in the experiments, $\xi_m \propto 1/\omega^2$ whence $D \propto 1/\omega^2$. For kb constant $\omega b(x)/v(x)$ is also constant and $\omega \propto v(x)/b(x)$. Therefore $D \propto b^2(d)/v^2(d)$. The jet flow into the pipe is $Q_j \propto Dv(d)$ and so the pipe flow, from Eq. (11), equal to the jet flow for volume drive and proportional to it for momentum drive so long as v_0 is constant, is

$$Q_p \propto b^2(d)/v(d). \tag{12}$$

For p_p constant this is a measure of the admittance. When the cutup is doubled, as in our experiments, the ratio of the admittances, from Eq. (12), is 5.9. In replotting the magnitudes, our data were adjusted by this factor.

The influence of v_0 can be simply catered for by a similar argument. If we consider a set of spirals having b constant, then, along a line of constant phase, k is an invariant function of x/d, whence, if similar steps are followed, the result follows that

$$Q_p \propto 1/v_0. \tag{13}$$

As a consequence of this result and for reasons which will become apparent, the magnitudes of the data from Fig. 6(a),(b) were replotted as $\log(v_0|Y|)$ vs $\log(\omega/v_0)$ and this is shown in Fig. 8. The points for $d = 2$ cm have been adjusted in the abscissa by the ratio involving the cutups $(0.02/0.01)^{3/2}$.

As was hoped, this method of portraying the results has a considerable simplifying effect. On the horizontal axis the values of $\log(\omega/v_0)$ are marked which correspond to the approximate boundaries between the three types of behavior found in the last section. Happily, these also mark the boundaries between three very obviously different trends in the data on this figure. Taking these in the same order as before, we examine the $\omega/v_0 \gtrsim 100$ range first.

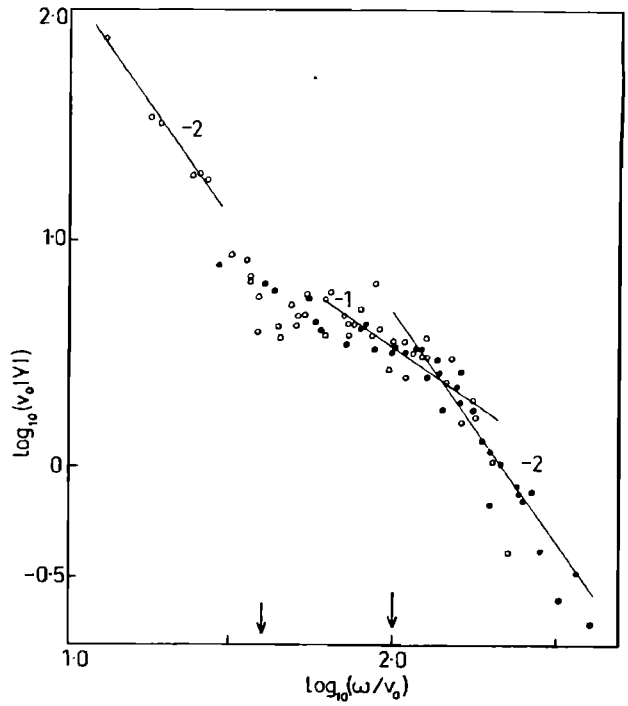

FIG. 8. The magnitudes of the jet admittances shown in Fig. 6(a),(b) replotted as $\log_{10}(v_0|Y|)$ vs $\log_{10}(\omega/v_0)$. ●-●-, $d = 2$ cm; O-O-, $d = 1$ cm. The solid lines, discussed in the text, are labeled with their slopes. The two arrows mark the boundaries of the various drive regimes defined in Sec. IV.

On the assumption that this is a volume drive regime, the expected form of $v_0|Y|$ as a function of ω and v_0 may be calculated from Eq. (11). This gives

$$v_0|Y| \propto Q_j v_0 \propto Dv_0^2. \tag{14}$$

If we write the jet tip deflection as $\mathscr{D}(\omega/v_0)\xi_m$ where the function $\mathscr{D}(\omega/v_0)$ incorporates the amount of growth in each case, then we have

$$v_0|Y| \propto (v_0/\omega)^2 \mathscr{D}(\omega/v_0). \tag{15}$$

The jet tip deflection as a function of ω and v_0 can be estimated numerically by integrating along a growth curve as given by Eq. (6). From such an integration we find that for $\omega/v_0 \lesssim 50$, $\mathscr{D}(\omega/v_0) \propto (\omega/v_0)^2$, for $50 \lesssim \omega/v_0 \lesssim 200$, $\mathscr{D}(\omega/v_0) \propto \omega/v_0$, and for $\omega/v_0 \gtrsim 200$, $\mathscr{D}(\omega/v_0)$ is almost independent of ω/v_0.

Using Eq. (15) we might predict from these trends that for $\omega/v_0 \gtrsim 100$, $v_0|Y| \propto v_0/\omega$, but that this should quickly change to $v_0|Y| \propto (v_0/\omega)^2$ for $\omega/v \gtrsim 200$. These correspond to the slopes of -1 and -2, respectively, in Fig. 8 as drawn. They describe the form of the data quite well. Should the drive still be in this regime at lower ω/v_0 values, the expected form of $\mathscr{D}(\omega/v_0)$ is now $\mathscr{D}(\omega/v_0) \propto (\omega/v_0)^2$. This causes $v_0|Y|$ to be independent of ω/v_0 and the curve in the figure should flatten further, which it does.

Turning now to the middle range, $40 \lesssim \omega/v_0 \lesssim 100$, the results in the last section suggested a transition from volume drive to a situation where momentum drive becomes important. At the opposite extreme to the volume drive case, that

is, one where momentum drive is dominant, the form of $v_0|Y|$, calculated from Eq. (11), is

$$v_0|Y| \propto v_0^3 \mathscr{D}(\omega/v_0)/\omega^2. \tag{16}$$

Here $\mathscr{D}(\omega/v_0) \propto (\omega/v_0)$ which gives for $v_0|Y|$, $v_0|Y| \propto v_0$, or $|Y|$ is constant. In Fig. 8 this predicts that the slope of each data set having v_0 constant should be zero but that the sets will separate according to the value of v_0. Although it is not really possible to tell whether this is happening or not in the figure, there is certainly sufficient scatter in the data on this level section to partly contain such a trend. Nevertheless, it appears unlikely. This is not surprising since the proportion of momentum drive for $\omega/v_0 \gtrsim 40$ is not very large. It must be remembered that there is really a mixture of the two drives and that, apart from this v_0 dependence, each of the extremes individually predicts a fairly minor variation of $v_0|Y|$ with ω/v_0, for the midrange, very much as the figure shows.

Since $c > 2.6v_0$ in Eq. (11), the other possibilities in this center range are that, for $\omega/v_0 \to 100$, the volume drive will dominate in the numerator, with $Z_p > Z_m$ in the denominator and, for $\omega/v_0 \to 40$, the momentum drive will dominate in the numerator with $Z_m > Z_p$ in the denominator. In this range $\mathscr{D}(\omega/v_0) \propto \omega/v_0$ so for the first possibility $v_0|Y| \propto v_0$ and for the second $v_0|Y|$ is constant. Thus for every possibility, the data in this midrange behave in a way which is consistent with the dictates of the simple theory. The effect of the change in Δl which has been, hitherto, ignored in this section, is necessarily small since, between the two data sets portrayed, it varies only from $\Delta l = 19$ cm to $\Delta l = 24$ cm.

So far, in this section, the admittance magnitude has followed the trends which we expected, but, as with the phase, we are left with the few data points for $\omega/v_0 \lesssim 40$ exhibiting a quite unexpected behavior. According to Eq. (11), the interaction should be largely momentum drive in this range. It has already been shown that at this extreme $|Y|$ is expected to be constant. This interpretation, while quite plainly not productive of the right answer, is erroneous anyway because, for ω/v_0 so small, the growth on the jet is no longer of material importance in determining the jet tip deflection. The acoustic displacement in the mouth is the important quantity.

In the limit, as $\omega d/u \to 0$, the expression for the jet deflection, Eq. (8) tends to $y(t) \to -(U_m x/u)\sin(\omega t - \pi/2)$, giving $D \propto 1/\omega v_0$. This yields $v_0|Y| \propto v_0/\omega$ for the magnitude of the admittance, corresponding to a slope of -1 in Fig. 8. The slope drawn through the data points on this part of the figure is -2, in considerable disagreement with this naive argument. Again, we can only conclude that some other physical mechanism is governing the interaction here.

VI. CONCLUSION

The jet–pipe interaction exhibits many features which can be explained with simple arguments and existing theories. Using the concept of a jet admittance, its dependence on D, ω, P_0, and Δl was investigated experimentally. For ω, P_0, and Δl constant, which eliminates variations in the drive mechanism, the admittance is roughly independent of D provided $D \lesssim 0.7b$. For larger deflections the admittance decreases as saturation in the jet flow occurs.

Using this small deflection regime, the admittance can be easily measured as a function of the drive parameters, ω, P_0, and Δl. The excitation of a pipe with a pulsating jet was first measured and found to be well characterized by the existing drive equation with a reweighting of the two terms, favoring momentum drive.

The jet admittance was then measured as a function of these drive parameters for a conventionally driven organ pipe. For $\omega/v_0 \gtrsim 40$, that is medium to high frequencies and medium to low blowing pressures, evidence of both the volume and momentum drive mechanisms was found in the phase and magnitude of the excitation. However, the drive equation needed to be further reweighted in favor of momentum drive, giving a coefficient of about 4 to the first term in Eq. (11).

For $\omega/v_0 \lesssim 40$ the phase and magnitude of the admittance both exhibit an entirely unexpected behavior. It is doubtful that this low-frequency, high blowing pressure trend could be described by any modification to the various terms in the drive equation, since the phenomenon occurs over far too small a range in ω/v_0 to be explained by any of the possible phase shifts in the equation. It does appear to be some quite different effect, not, as yet, included in any theoretical considerations of the problem.

ACKNOWLEDGMENTS

This paper is part of a program in musical acoustics which is supported by the Australian Research Grants Scheme. Suszanne Thwaites is indebted to the University of New England for the award of a Research Scholarship.

[1] L. Cremer and H. Ising, "Die selbsterregten Schwingungen von Orgelpfeifen," Acustica **19**, 143–153 (1967).
[2] J. W. Coltman, "Sounding mechanism of the flute and organ pipe," J. Acoust. Soc. Am. **44**, 983–992 (1968).
[3] S. A. Elder, "On the mechanism of sound production in organ pipes," J. Acoust. Soc. Am. **54**, 1554–1564 (1973).
[4] N. H., Fletcher, "Nonlinear interactions in organ flue pipes," J. Acoust. Soc. Am. **56**, 645–652 (1974).
[5] J. W. Coltman, "Jet drive mechanisms in edge tones and organ pipes," J. Acoust. Soc. Am. **60**, 725–733 (1976).
[6] N. H. Fletcher, "Transients in the speech of organ flue pipes—a theoretical study," Acustica **34**, 224–233 (1976).
[7] N. H. Fletcher, "Jet-drive mechanism in organ pipes," J. Acoust. Soc. Am. **60**, 481–483 (1976).
[8] N. H. Fletcher, "Sound production by organ flue pipes," J. Acoust. Soc. Am. **60**, 926–936 (1976).
[9] N. H. Fletcher, "Mode locking in nonlinearly excited inharmonic musical oscillators," J. Acoust. Soc. Am. **64**, 1566–1569 (1978).
[10] N. H. Fletcher and L. M. Douglas, "Harmonic generation in organ pipes, recorders, and flutes," J. Acoust. Soc. Am. **68**, 767–771 (1980).
[11] H. L. F. Helmholtz, *On the Sensations of Tone as a Physiological Basis for the Theory of Music*, (1877) (Translated by A. J. Ellis and reprinted by Dover, New York, 1954), pp. 92–93.
[12] Lord, Rayleigh, *The Theory of Sound*, (1896) (reprinted by Dover, New York, 1945), Vol. 2, pp. 218–220.
[13] J. W. Coltman, "Momentum transfer in jet excitation of flutelike instruments," J. Acoust. Soc. Am. **69**, 1164–1168 (1981).
[14] N. H. Fletcher and S. Thwaites, "Wave propagation on an acoustically perturbed jet," Acustica **42**, 323–333 (1979).
[15] S. Thwaites and N. H. Fletcher, "Wave propagation on turbulent jets," Acustica **45**, 175–179 (1980).
[16] S. Thwaites and N. H. Fletcher, "Wave propagation on turbulent jets: II, Growth," Acustica **51**, 44–49 (1982).
[17] L. E. Kinsler and A. R. Frey, *Fundamentals of Acoustics* (Wiley, New York, 1962), pp. 134–136.